Replication of Flows in A Pipe Network of Sprinkler Irrigation System Using Ansys-CFD

Abstract: Sprinkler irrigation plays an important role in distributing water effectively for agricultural fields with the aid of a network of pipes and outlets efficiently. The study focuses on addressing the hydraulic behavior of the flow for sprinkler systems without nozzles using Ansys-CFD. The primary objectives include examining the flow distribution in the laterals of the sprinkler system, studying the relationship between pipe diameter and flow velocity, and determining the pipe size for uniform flow. By analyzing the flow patterns and pressure variations the study aims to improve the efficiency of water application.. This study examines flow distribution in the laterals of the sprinkler system through numerical simulation. The methodology involves conducting numerical simulations using Ansys fluent, 3D model is analyzed for flow pattern and pressure variation in the pipe network in sprinkler irrigation system. The present study emphasizes the relationship between the diameter of the pipe and the velocity of the flow. As a consequence of this, the requirement of selecting a suitable pipe diameter to ensure uniform flow can be achieved. Analytical estimations were used to compare the accuracy of the numerical simulation, revealing a good agreement between them with an error margin of 5%. These results contribute valuable insights into the design and functionality of sprinkler systems, particularly in optimizing flow uniformity and water conservation.

Keywords*: Sprinkler network, Irrigation, Ansys-CFD, pipe diameter, velocity, and pressure distribution.*

1. Introduction

The sprinkler networks play a vital tool for conserving resources and optimizing agricultural output. This sprinkler network system is used in agriculture to deliver water directly to the plant root zone. It consists of a pipe network system and sprinkler heads. The effectiveness of this method is to reduce water wastage and uniform water distribution to the larger fields [1] and provide consistent hydration. These systems allow high productivity with less water. In addition to water management, sprinkler systems offer flexibility and adaptability. This system permits the farmers to vary watering schedules and regulate them based on the requirement of crop needs, changes in the weather, and soil conditions. The pipe network is constructed with durable materials and is built to continue prolonged use and significant environmental conditions, involving minimal maintenance over time. While they are highly efficient in delivering water and have financial constraints, the cost of installation is high, and weather pattern sensitivity challenges, especially in areas with variable water and power supplies. Nonetheless, sprinkler network systems remain a sustainable solution for improving agricultural yield while managing water resources effectively. Typically, a sprinkler setup or system includes a pump and, a network of pipes consisting of a main, laterals, and sprinklers [2]. A typical layout is depicted in Fig. 1.

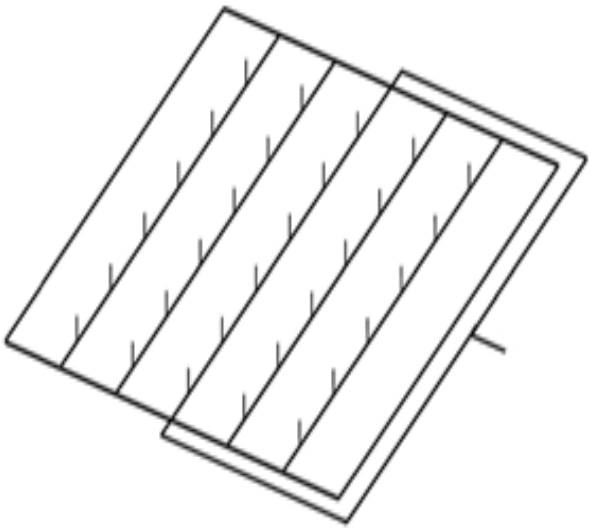

Fig. 1. Typical sketch of sprinkler network system

2. Literature review

Several studies have delved into improving irrigation systems through technological advancements. Zhu [3-4] focused on soil moisture sensors for irrigation, highlighting the use of distributed wireless sensor networks and real-time data management to improve irrigation efficiency. Their work emphasized the importance of advanced sensor technology and remote communication for better irrigation decisions and future agricultural applications.

The study showed strong agreement between theoretical analysis, experiments, and simulations in predicting the flow-pressure relationship and jet behaviour [5]. Tang [6] conducted a 3D numerical simulation to evaluate the forces caused by water jet impact on a driving spoon in irrigation systems. The study found that CFD simulations were accurate under high-pressure conditions and had a 5% difference when corrected with experimental results, validating CFD's application in irrigation design. Guedaouria analyzed the irrigation systems for a semi-arid region, comparing drip and sprinkler designs. They found that a 15 l/h dripper was the most efficient solution for reducing water and energy usage. Installing one larger pump with a pressure reducer was recommended for optimized system performance [7].

Mateos investigated the design and failures of sprinkler nozzles, recommending brass as the optimal material for nozzle manufacturing based on Finite Element Analysis [8]. The effective performance of brass nozzles and reliability under 2.0 kg/cm^2 pressure conditions [9]. The effects of pressure fluctuations are studied in pressurized irrigation systems, using a stochastic simulation model by Daccache [10]. The study showed that, pressure fluctuations or changes significantly affect the uniformity of water distribution and improvement in the network with a 5% error between experimental and numerical simulation results using Ansys-CFD. Using a stochastic simulation model, the study investigated the impact of pressurized distribution systems in calculating hydrant pressure under varying conditions of on-farm sprinkler network performance [11]. An iterative model was developed to generate the characteristic curves of both the on-farm network and hydrants by Trung. The analysis revealed that, fluctuations in hydrant pressure significantly affect the performance of the sprinkler system [12].

In view of the above literature and results, In the present study, the pipe diameter is kept larger than the nominal diameter. This is due to the fact that solids in the flow may settle down in the conduit and reduce the effective cross-sectional area of the pipe. Therefore, simulation studies were targeted to ascertain the flow distribution in all the laterals. Moreover, it is also aimed at verifying whether the flow is moving with the same velocity from either side of the lateral or not. Hence, the present study intends to determine the flow velocity at all the outlet points. The present investigation was conducted for a wastewater treatment plant having a flow rate of 5206 l/hr without any sprinkler heads. The laterals were spaced 1.0 m apart, while the main pipeline had a diameter of 75 mm. The diameter of the lateral pipe was 50 mm and 25 mm, and the rise of the sprinkler head was 127 mm. The discharge through a sprinkler nozzle can be computed from the orifice flow formula that is given as CAV, and the dynamic pressure can be computed from ($0.5\rho V^2$) where Q = total discharge through all the nozzles in cumec, A = cross-sectional area of the nozzle in sq. m., V = flow velocity through the nozzle in m/s, C = coefficient that accounts for losses in the system = 0.96.

3. Computational model

3.1. Basic Principle of closed flow

According to Bernoulli's law for closed flow systems [1], the pressure in the inlet pipe can be calculated. The necessary parameters for

calculating the inlet pipe pressure are the total head between the inlet and outlet pipes and the pipe diameter to be used.

$$P_1 + \frac{1}{2}\rho v_1^2 + \rho g h_1 = P_2 + \frac{1}{2}\rho v_2^2 + \rho g h_2 \quad \ldots\ldots(1)$$

In piping systems, pressure measurement must account for the total head, pipe diameter, and head losses, which include major losses (due to fluid viscosity, velocity, and pipe roughness) and minor losses (from fittings, valves, and pipe reductions) which can be neglected in some cases [2]. The major head loss was calculated using the below equation.

$$H_L = f\frac{L}{d}\frac{v^2}{2g} \quad \ldots\ldots(2)$$

Where f is the friction factor, L is the length of the pipe, d is the diameter of the pipe, v is the average fluid velocity, and g is the acceleration due to gravity.

3.2 Governing equations for single phase flow in CFD

For single-phase flow simulations in a sprinkler network system using ANSYS Fluent the governing equations [13] typically include:

Continuity equation: This equation represents the conservation of mass and ensures that mass is conserved within the flow domain.

$$\nabla \cdot v = 0 \quad \ldots\ldots(3)$$

where ρ is the density of the fluid and v is the velocity vector field.

Navier-Stokes equations: These equations describe the conservation of momentum and govern the fluid flow behaviour.

$$\rho\left(\frac{\partial v}{\partial t} + (v\nabla)v\right) = \nabla_p + \nabla(\mu(\nabla v + (\nabla v + (\nabla v)^T) - \nabla(\rho\overline{u'v'}) + f \quad \ldots\ldots(4)$$

Where t is time, p is the pressure, μ is the dynamic viscosity, u′v′ represents the Reynolds stresses (turbulent stresses), which are modeled using the turbulence model, and f represents any external body forces acting on the fluid [14].

In this k-epsilon turbulence model, two additional transport equations for the turbulent kinetic energy k and the turbulent dissipation rate ε.

k-equation: This equation represents the turbulent kinetic energy and accounts for the turbulent fluctuations in velocity [10].

$$\frac{\partial(\rho k)}{\partial t} + \nabla.(\rho k v) = \nabla.\left[\left(\frac{\mu_t}{\sigma_k} + \frac{\rho v_t}{\sigma_k}\right)\nabla k\right] + p_k - \rho\varepsilon \quad \ldots\ldots(5)$$

ε-equation: This equation describes the turbulent dissipation rate and governs the rate at which turbulence kinetic energy is dissipated into heat.

$$\frac{\partial(\rho\varepsilon)}{\partial t} + \nabla.(\rho\varepsilon v) = \nabla.\left[\left(\frac{\mu_t}{\sigma_\varepsilon} + \frac{\rho v_t}{\sigma_\varepsilon}\right)\nabla\varepsilon\right] + C_{1\varepsilon}\frac{\varepsilon}{k}p_k - C_{2\varepsilon}\rho\frac{\varepsilon^2}{k} \quad \ldots\ldots(6)$$

where μ_t is the turbulent viscosity, P_k denotes the production of turbulent kinetic energy, and $C_{1\varepsilon}$ and $C_{2\varepsilon}$ are model constants. The model also involves constants σ_k and σ_ε to stabilize the equations [15]. The mainly used model is k–ε turbulence model is particularly suitable for a wide range of flow conditions. It is a popular selection for simulating turbulent flows, including those encountered in sprinkler network systems.

3.3 Procedure of the fluent CFD

CFD procedure involves many steps to ensure accurate and reliable results [16]. In this, there are three Phases viz., pre-processing, processing, and post-processing. The pre-processing begins with the geometry where the 3D model is generated using design modular in ANSYS. A fine mesh is created to discretize the geometry and assign suitable boundary conditions to the geometry. The symmetry boundary condition is used in the study which reduces the computational domain by exploiting geometric and loading symmetry condition for enhancing computational efficiency. This approach ensures accurate results by modeling only a representative section of the system. The next phase, processing involves selecting an appropriate solver, such as the k-ε model, to compute the flow characteristics based on well-defined parameters. The convergence criterion was set to $1*10^5$ or below it for the accuracy of the solution. The above value was employed to observe the residuals for continuity and momentum throughout the simulation. Subsequently, the post-processing allows for the detailed analysis of results, including flow pattern visualization and data extraction.

The last step is the validation, where the CFD results are compared with analytical values to assess the model's accuracy as shown in Fig. 2. If any differences are found, then adjustments are made to improve the geometrical model,

ensuring a comprehensive analysis and dependable outcomes in fluid dynamics research. This structured approach is necessary for advancing the reliability of CFD applications.

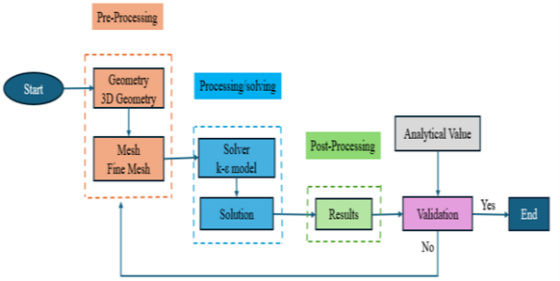

Fig. 2. Procedure of the ANSYS-CFD

4. Simulation of Sprinkler Network System

The 3D model of the computational domain was developed using design modular in Ansys Workbench. The full geometry can be efficiently generated by modelling only half of the domain, as the other half is a symmetrical mirror of it [16]. This approach reduces computational complexity, shortens convergence time, and improves accuracy by leveraging symmetry in the simulation without sacrificing analytical precision. The simulation was conducted for varying pipe diameters as shown in Fig.3(a) illustrates the geometry of a 50 mm diameter pipe, while Fig. 3(b) shows a 25 mm diameter pipe.

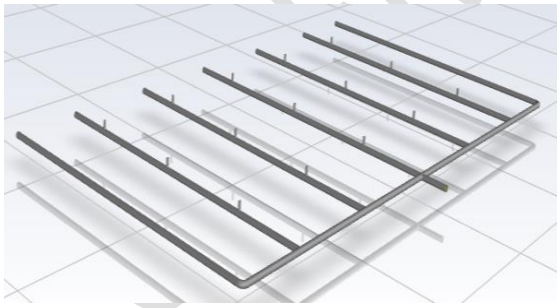

(a)

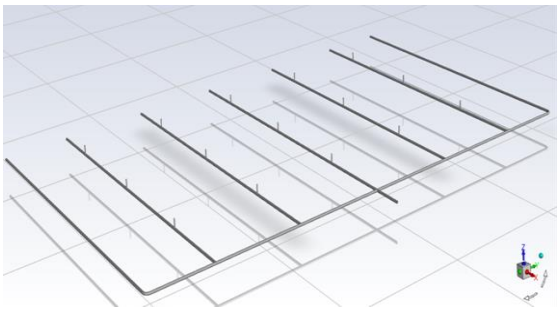

(b)

Fig. 3. (a) Geometry of 50 mm pipe network and (b) 25 mm pipe network

Subsequently, the entire fluid domain was discretized, leading to the generation of the structured mesh [17]. In the process, the mesh was made very fine as shown in Fig. 4(a) and (b). The fluid domain was discretized for a 50 mm pipe diameter with 4,97,586 mesh elements and the number of nodes as 51,565. The mesh elements are 4,47,559 and number of nodes is 1,06,334 for 25 mm. The mesh minimum orthogonal quality was 0.89 in both pipe cases. The mesh was then imported into Fluent setup, where the simulation was allowed utilizing single-phase flow analysis.

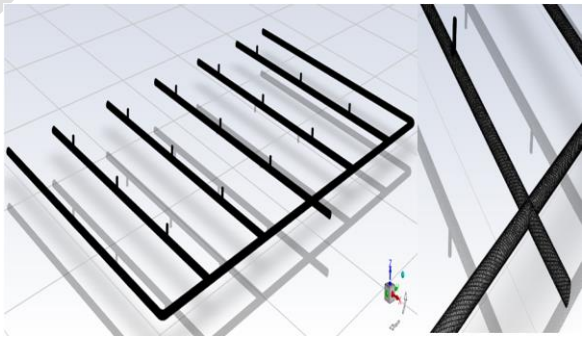

(a)

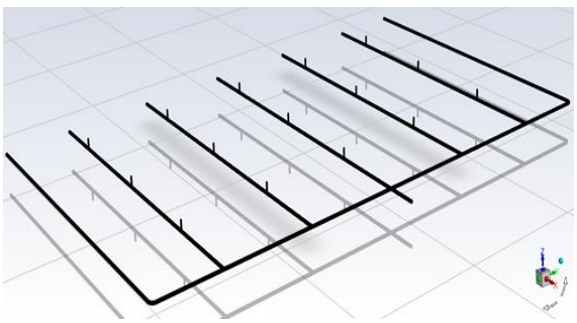

(b)

Fig. 4. (a) Meshing of 50 mm pipe network and (b) 25 mm pipe network

The boundary conditions for the sprinkler network include a velocity inlet and a pressure outlet, with symmetrical boundary conditions applied at the ends of all lateral pipes [18]. The remaining geometrical boundaries are defined as walls and are depicted in Fig. 5 (a) and (b) for both pipe diameters. Symmetrical boundary conditions are used when the physical shape and anticipated flow pattern exhibit mirror symmetry, streamlining the simulation process.

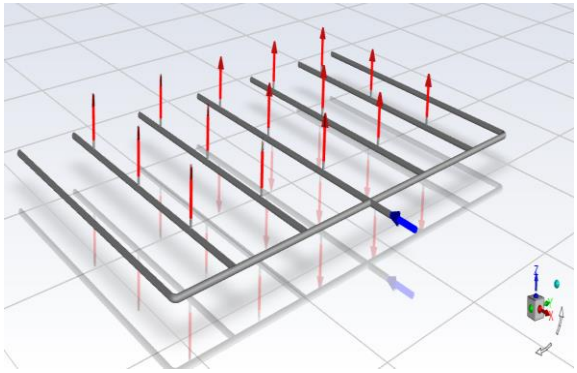

(a)

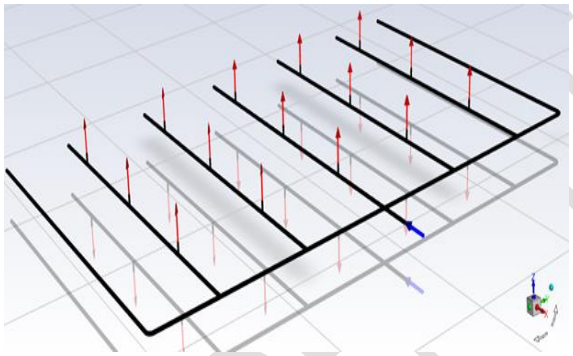

(b)

Fig. 5. (a) Boundary Description for 50 mm pipe diameter and (b) 25 mm pipe diameter

The next step is to initialize the solution. The number of time steps is to be set, and the size of the step to be taken is to get absolute criteria for convergence as shown in Fig. 6(a) and (b). The solution procedure was extended till it converged to satisfy the required flow pattern up-to the symmetry of the sprinkler network.

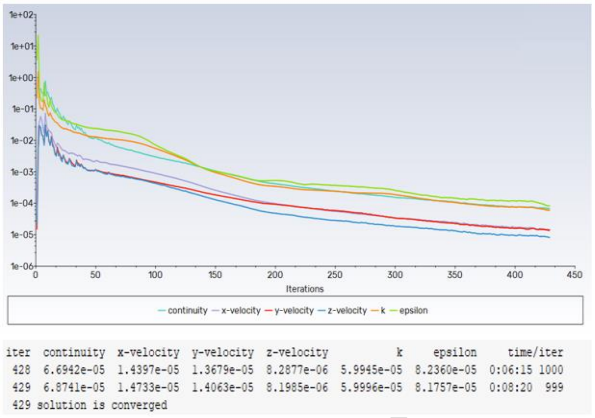

iter	continuity	x-velocity	y-velocity	z-velocity	k	epsilon	time/iter	
428	6.6942e-05	1.4397e-05	1.3679e-05	8.2877e-06	5.9945e-05	8.2360e-05	0:06:15	1000
429	6.8741e-05	1.4733e-05	1.4063e-05	8.1985e-06	5.9996e-05	8.1757e-05	0:08:20	999
429 solution is converged								

(a)

Fig. 6. (a) Iteration graph for 50 mm pipe network

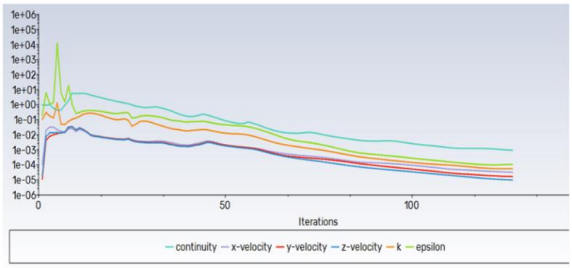

iter	continuity	x-velocity	y-velocity	z-velocity	k	epsilon	time/iter	
126	9.7779e-04	3.3542e-05	1.7302e-05	1.0188e-05	5.5793e-05	1.0727e-04	0:00:00	100
126 solution is converged								
127	9.2146e-04	3.2225e-05	1.6504e-05	9.8268e-06	5.5266e-05	1.0758e-04	0:01:39	99
127 solution is converged								

(b)

Fig. 6 (b) Iteration graph for 25 mm pipe network

Contours of dynamic pressure in CFD are graphical representations that illustrate the distribution of dynamic pressure across a fluid domain. Dynamic pressure is a measure of the kinetic energy per unit volume of a fluid and is a main parameter in fluid flow analysis. Contour plots of dynamic pressure use contour lines to represent variations in pressure within the fluid as shown in Fig. 7(a) and (b) for pipe diameters of 50 and 25 mm.

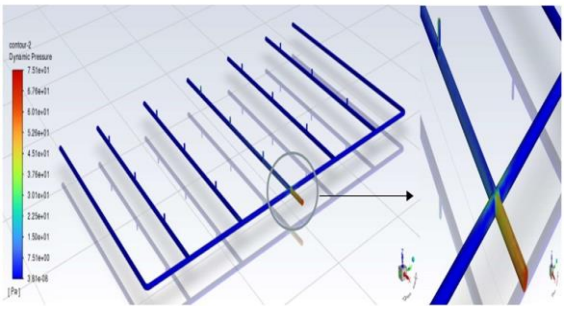

(a)

Fig. 7. (a) Contours of Dynamic Pressure for 50 mm pipe network

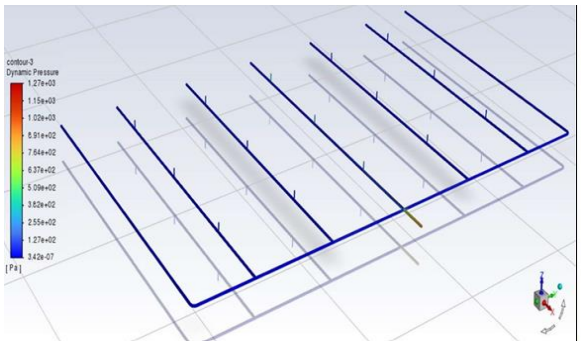

(b)

Fig. 7. (b) Contours of Dynamic Pressure for 25 mm pipe network

Velocity magnitude is a scalar field that represents the magnitude or speed of the fluid's velocity at each point within the domain [19]. In CFD simulations, this is often depicted using contour plots where different colors or contour lines indicate variations in velocity magnitude of both the pipe networks of 50 and 25 mm as depicted in Fig. 8.

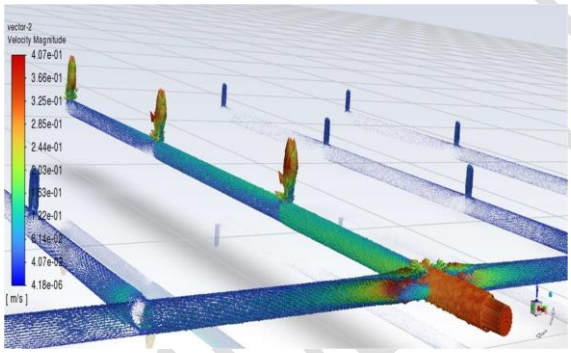

Fig. 8. Contours of Velocity Magnitude for 50 mm pipe network

Velocity vectors are vector fields that provide information about both the speed and direction of fluid flow at specific enlarged locations within the domain as shown in Fig. 9.

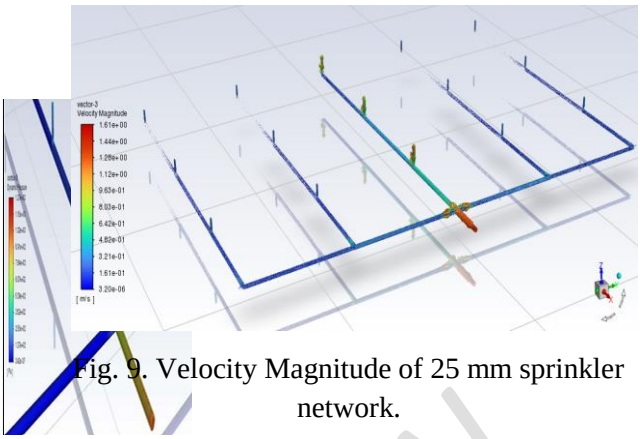

Fig. 9. Velocity Magnitude of 25 mm sprinkler network.

These vectors are typically represented as arrows or lines, with the length of the arrow indicating the velocity magnitude and the direction of the arrow indicating the flow direction. The various hydraulic parameters, viz., velocity magnitude, dynamic Pressure, and mass flow rate, were obtained in a 50 mm and 25 mm pipe network. The simulated values for these parameters are presented in Table 1.

Table 1. Simulation Values for pipe networks of 50 mm diameter

Parameters	Velocity Magnitude (m/s)	Dynamic Pressure (MPa)	Mass flow rate (kg/s)
Inlet_1	0.35675	63.2745	0.3549751
Inlet_2	0.35675	63.2745	0.3549751
Outlet11	0.064343	2.185149	0.0319125
Outlet12	0.0629698	2.058794	0.0312468
Outlet13	0.0630736	2.050857	0.0313847
Outlet14	0.0630736	2.050857	0.0313847
Outlet15	0.0629698	2.058794	0.0312468
Outlet16	0.0643435	2.185149	0.0319125
Outlet21	0.0590164	1.846526	0.0292908
Outlet22	0.0569375	1.685826	0.0282534
Outlet23	0.0565626	1.662141	0.0281691
Outlet24	0.0565626	1.662141	0.0281691
Outlet25	0.0569375	1.685826	0.0282534
Outlet26	0.0590164	1.846526	0.0292908
Outlet31	0.2229805	27.38252	0.0554308
Outlet32	0.2354645	29.26254	0.0584504
Outlet33	0.2444244	30.45039	0.0607212
Outlet34	0.2444244	30.45039	0.0607212
Outlet35	0.2354645	29.26254	0.0584504
Outlet36	0.2229805	27.38252	0.0554308

Outlet41	0.0590164	1.846526	0.0319125
Outlet42	0.0569375	1.685826	0.0312468
Outlet43	0.0565626	1.662141	0.0313847
Outlet44	0.0565626	1.662141	0.0313847
Outlet45	0.0569375	1.685826	0.0312468
Outlet46	0.0590164	1.846526	0.0319125
Outlet51	0.0643435	2.185149	0.0319125
Outlet52	0.0629698	2.058794	0.0312468
Outlet53	0.0630736	2.050857	0.0313847
Outlet54	0.0630736	2.050857	0.0313847
Outlet55	0.0629698	2.058794	0.0312468
Outlet56	0.0643435	2.185149	0.0319125

The velocity magnitude, dynamic pressure, and mass flow rate were determined for a pipe network with diameters of 25 mm. The simulated values for these parameters are presented in Table 2 for the 25 mm pipe.

Table 2. Simulation Values for pipe networks of 25 mm diameter

Parameters	Velocity Magnitude (m/s)	Dynamic Pressure (MPa)	Mass flow rate (kg/s)
Inlet_1	1.42698	999.648	0.3516670
Inlet_2	1.42698	999.648	0.3516670
Outlet11	0.310091	48.7731	0.0350470
Outlet12	0.302590	45.9542	0.0341742
Outlet13	0.300576	45.1506	0.0339636
Outlet14	0.300576	45.1506	0.0339636
Outlet15	0.302590	45.9542	0.0341742
Outlet16	0.310091	48.7731	0.0350470
Outlet21	0.286141	41.3744	0.0328040
Outlet22	0.281228	39.7518	0.0317655
Outlet23	0.279902	39.2451	0.0320233
Outlet24	0.279902	39.2451	0.0320233
Outlet25	0.281228	39.7518	0.0317655
Outlet26	0.286141	41.3744	0.3280400
Outlet31	0.888298	398.705	0.0504309
Outlet32	0.896887	403.189	0.0508577
Outlet33	0.914311	417.508	0.0513533
Outlet34	0.914311	417.508	0.0513533
Outlet35	0.896887	403.189	0.0508577
Outlet36	0.88829	398.705	0.0504309
Outlet41	0.286141	41.3744	0.0328040
Outlet42	0.281228	39.7518	0.0317655
Outlet43	0.279902	39.2451	0.0320233
Outlet44	0.279902	39.2451	0.0320233
Outlet45	0.281228	39.7518	0.0317655
Outlet46	0.286141	41.3744	0.3280400
Outlet51	0.310091	48.7731	0.0350470
Outlet52	0.302590	45.954	0.0341742
Outlet53	0.300576	45.1506	0.0339636
Outlet54	0.300576	45.1506	0.0339636
Outlet55	0.302590	45.9542	0.0341742
Outlet56	0.310091	48.7731	0.0350470

The comparison of both analytical and simulation values with the percentage of error for hydraulic parameters for the 50 mm and 25 mm pipe network is shown in Table 3. In the 50 mm lateral pipe network, the velocity at the point of entry is significantly higher compared to the rest of the laterals, leading to non-uniform flow distribution along the pipe length. This inconsistency in velocity distribution can result in inefficient application performance and unequal water delivery. In contrast, reducing the pipe diameter to 25 mm provides a more balanced flow across the network. The reduction in diameter helps to regulate the flow velocity along the length of the laterals, improving uniformity in water distribution. The modifications reveal that the required objectives, such as attaining consistent flow in the pipe laterals and optimizing the performance of the system, are achieved with the 25 mm network of the pipe, addressing the issues observed with the 50 mm configuration.

Table 3. Errors percentage in both pipe networks of 50 mm and 25 mm

Parameter	50 mm Pipe network		25 mm Pipe network	
	Velocity (m/s)	Dynamic Pressure (Pa)	Velocity (m/s)	Dynamic Pressure (Pa)
Analytical Values	0.20	6.77	0.401	111

Simulation Values	0.207	7.03	0.4145	115
% Error	3.65	3.39	3.36	3.60

5. Conclusions

The study addressed selecting the appropriate diameter of the pipe in the network to maintain the uniform flow distribution across all laterals in the system. A comparison made between the 50 mm and 25 mm diameters of the pipe networks showed that the larger diameter resulted in flow disagreements, while the smaller diameter achieved the required flow uniformity throughout the network system. The sprinkler lateral was analyzed through the numerical simulation using Ansys CFD to assess the velocity distribution along the laterals for each outlet. Initially, the sprinkler network with 50 mm diameter pipes is simulated revealing non-uniform flow viz., velocity and dynamic pressure across the laterals and outlets. To overcome this issue, the study proposed that the diameter of the pipe of 25 mm be simulated and found that a flow velocity of 0.4 m/s is ensured in all laterals for uniform flow distribution. The pipe of 25 mm diameter simulation proved consistent velocity and pressure throughout the system, ensuring uniform flow in all laterals and outlets. Analytical estimates are validated with the numerical simulations, showing a good agreement with a margin of error within 5% [20].

This study was conducted on a wastewater treatment plant with a flow rate of 5206 l/hr, excluding sprinkler heads. To avoid the entry of solids into the sprinkler pipe network, the findings also recommend the installation of a plate settler followed by a disc filter in the primary treatment unit of water recycling systems. Overall, this research shows the effectiveness of the numerical simulation in enhancing the sprinkler system performance, particularly in recognizing the suitable pipe diameters for attaining uniform flow distribution across all the outlets in the network, which is challenging to determine through physical modeling alone.

References

[1] S. K. Garg, "Irrigation Engineering and Hydraulic Structures," Khanna Publishers, Standard Book House, pp. 1-16, 2010.

[2] R. S. Varshney, "Theory & Design of Irrigation Structures, Canals and Storage Works," 4th ed., vol. 2, New Chand & Bros., Roorkee, pp. 134-145, 1988.

[3] X. Zhu, X. Wang, and J. Liu, "Numerical Simulation of a New Typed Sprinkler Irrigation System," Joint Fluids Engineering Conference, vol. 1, no. 1, pp. 3841-3845, 2011, doi: 10.1115/AJK2011-24006.

[4] X. Zhu, P. Chikangaise, W. Shi, W. H. Chen, and S. Yuan, "Review of intelligent sprinkler irrigation technologies for a remote autonomous system," International Journal of Agricultural and Biological Engineering, vol. 11, no. 1, pp. 23-30, 2018, doi: 10.25165/j.ijabe.20181101.3557.

[5] S. Yuan, X. Zhu, H. Li, et al., "Numerical simulation of inner flow for complete fluidic sprinkler using computational fluid dynamics," Transactions of the CSAM, vol. 36, no. 10, pp. 46-49, 2005.

[6] P. Tang, H. Li, Z. Issaka, and C. Chen, "Impact forces on the drive spoon of a large cannon irrigation sprinkler: Simple theory, CFD numerical simulation and validation," Biosyst. Eng., vol. 159, pp. 1-9, 2017, doi: 10.1016/j.biosystemseng.2017.04.005.

[7] H. Guedaouria, M. Daoudi, Y. Benmoussa, and A. Maazouzi, "Irrigation Network Requirements for Watering Urban Green Space in Semiarid Region," IOP Conf. Ser.: Earth Environ. Sci., vol. 973, pp. 1-7, 2022, doi: 10.1088/1755-1315/973/1/012013.

[8] L. A. Mateos, "A Simulation study of comparison of the evaluation procedures for three irrigation methods," Irrigation Science, vol. 25, pp. 75-83, 2006.

[9] S. T. Warghat, K. P. Kawatkar, and D. V. Astonkar, "Investigation & improvement of the performance of sprinkler nozzle by using FEM," Int. Res. J. Eng. Technol., vol. 6, no. 4, pp. 23-27, 2019.

[10] A. Daccache, N. Lamaddalena, and U. Fratino, "On-demand pressurized water distribution system impacts on sprinkler network design and performance," Irrig. Sci., vol. 28, no. 4, pp. 331-339, 2010, doi: 10.1007/s00271-009-0195-7.

[11] N. Lamaddalena, U. Fratino, and A. Daccache, "On-farm Sprinkler Irrigation Performance as affected by the Distribution System," Biosyst. Eng., vol. 96, no. 1, pp. 99-109, 2007, doi: 10.1016/j.biosystemseng.2006.09.002.

[12] M. C. Trung, S. Nishiyama, and H. Anyoji, "Application of unsteady flow analysis in designing a multiple outlets sprinkler irrigation system," Paddy Water Environ., vol. 5, pp. 181-187, 2007.

[13] W. Y. Tey, N. A. Sidik, Y. Asako, and R. Z. Goh, "Governing equations in computational fluid dynamics: Derivations and a recent review," Progress Energy Environ., vol. 1, pp. 1-19, 2017.

[14] H. K. Versteeg and W. Malalasekera, "An Introduction to computational fluid dynamics," 2nd ed., pp. 80-111, 2007.

[15] Y. Hassan, "An overview of computational fluid dynamics and nuclear applications," Thermal-Hydraulics of Water-Cooled Nuclear Reactors, Elsevier, pp. 729-829, 2017, doi: 10.1016/B978-0-08-100662-7.00012-9.

[16] Ansys Fluent Workbench Tutorial Guide, 2021 R2.

[17] N. S. Ramya and N. S. Kumar, "Analysis and Simulation of Flow over Stepped Spillway Using Ansys-CFD," Asian Research Journal of Current Science, vol. 5, no. 1, pp. 155-162, 2023.

[18] S. V. S. N. D. L. Prasanna and N. Suresh, "Estimation and Simulation of Flows into an off-Taking Canal Using ANSYS," Advanced Modelling and Innovations in Water Resources Engineering, Springer Nature Singapore, 2024, doi: 10.1007/978-981-16-4628-7.

[19] S. N. Ramya, M. M. Reddy, S. V. Reddy, R. S. Kumar, and D. Tanuja, "A Comprehensive approach using CFD and GIS for dam break risk analysis: A case study on Nagarjuna Sagar earthen dam," Disaster Advances, vol. 17, no. 3, pp. 35-47, 2024, doi: 10.22606/dad.2024.170304.

[20] ISO 5725-1:1994, "Accuracy (trueness and precision) of measurement methods and results - Part 1: General principles and definitions."